

# DFT study on the adsorption mechanism of 2-butyne-1,4-diol on the Fe(100) surface as a corrosion inhibitor for steel pickling

Hermine Schmidtbauer, Peter Blaha, Herbert Danninger, and Bernhard Mayr-Schmölzer  
*Institute of Materials Chemistry, Vienna University of Technology,  
Getreidemarkt 9/165-TC, A-1060 Vienna, Austria*

## Abstract

The electronic interaction of the corrosion inhibitor molecule 2-butyne-1,4-diol with the (100) surface of Fe(bcc) is modelled in a density functional theory (DFT) approach. Using periodic surface slabs the adsorption energies of various adsorption sites are calculated and the adsorption mechanism of the inhibitor to the steel surface is resolved. Furthermore, the interaction of the adsorbate with a water molecule via hydrogen bond formation to the molecule's hydroxyl group is shown. We observe covalent bonds and a backbonding character between iron atoms and the alkyne group. The most favourable adsorption geometry is found having the unsaturated bond in a fourfold di- $\sigma$  position with an angle of almost  $45^\circ$  to the Fe[100] direction. Both the geometric properties and the presence of remaining  $\pi$ -character electronic states indicate a reduced double bond character of the adsorbed molecule. The mechanism can be classified as chemisorption, due to the chemical change of the adsorbate and the high adsorption energy.

PACS numbers: 71.15.Mb, 68.43.Bc, 68.43.Fg, 81.65.Kn

## I. INTRODUCTION

In technological steel production red-hot steel slabs are hot-rolled and cooled down afterwards in air. Under these ambient conditions the hot steel sheet gets oxidised by atmospheric oxygen, and scale, layers of the iron oxides wuestite ( $\text{Fe}_{1-x}\text{O}$ ), magnetite ( $\text{Fe}_3\text{O}_4$ ) and haematite ( $\text{Fe}_2\text{O}_3$ ), forms on the surface. The brittle oxide layers have to be removed before further processing, thus, the steel sheet is pickled in a hydrochloric acid bath. While scale is dissolved through an acid corrosion mechanism, the removal of bulk steel should be prevented by adding a corrosion inhibitor to the acid solution. In that way, large quantities of material loss can be saved in steel production during the process of pickling by the use of corrosion inhibitors. The present work models the principle of inhibitor - metal interaction of the alkynol 2-butyne-1,4-diol as an active substance in the commercially available corrosion inhibitor Adacid VP11 in a density functional theory (DFT) approach. The findings enable one to understand basic concepts and to apply these to process development and -improvement in the future.

Quantum chemical calculations have become widely used to study the electronic structure and reactivity of corrosion inhibitor molecules. In a recent review, Gece<sup>1</sup> gives an overview of tens of theoretical studies on different inhibitor substances trying to find correlation between quantum chemical properties and the inhibitor efficiency. Such a theoretical study has also been carried out on the adsorption mechanism of the alkynol inhibitor molecule 1-propyn-3-ol using the Gaussian 94 package by Lendvay-Györik<sup>2</sup>. Two different possible binding sites on one single Fe atom were suggested, namely the hydroxyl group, forming an O-bonded adsorbate, and the C-C triple bond  $\pi$ -system. The study resulted in a preferred bond between the unsaturated group and Fe, which is what we verify by modelling a periodic solid surface in-

stead of just a single Fe atom, thus, we expect higher accuracy, applying WIEN2k rather than the Gaussian package on solid systems.

The formation of covalent bonds between the alkynolic inhibitor and iron has not always been known. In prior studies a polymerisation mechanism of  $\pi$ -bonded alkynols on steel was suggested to explain the vanishing  $\text{C}\equiv\text{C}$  vibration band in IR-spectra after adsorption<sup>3,4,5</sup>. In the contrast, the vanishing  $\text{C}\equiv\text{C}$  band was afterwards explained with the formation of a covalent bond to the metal surface, *i.e.* a reduction of the bond order from a triple bond into a double bond<sup>6</sup>. In agreement to Lendvay-Györik<sup>2</sup>, a chemisorption mechanism of alkynols on iron via the alkyne group and the oxygen lone pair were further on suggested by molecular modelling and XPS analysis<sup>7</sup>. In the present study we verify the chemisorption mechanism via the alkyne group, thus the weakening of the bond order in 2-butyne-1,4-diol.

When choosing the Fe surface plane for the surface slab model, we consider the following: The surface energy of Fe planes is, typical for bcc transition metals, in the order of  $E(110) < E(100) < E(111)$ <sup>8</sup>, thus the most stable plane would be Fe(110). But since stable acetylene adsorption was found on each of these planes, and the order of interaction was stated  $(100) > (110) > (111)$  (using molecular orbital theory)<sup>9</sup>, the Fe(100) plane would yield strongest adsorption of alkyne groups (as in acetylene and the investigated substance 2-butyne-1,4-diol). Therefore, and in particular for computational reasons (highest symmetry), we choose the Fe(100) plane as a model surface in the present work. We want to mention that all the differently oriented crystal planes have to be covered by the inhibitor for areawide steel surface protection and a consequential inhibiting effect. Furthermore, inhibitor adsorption in aqueous medium is only possible if the inhibitor has a higher tendency to adsorb on iron than water, in which the attacking acid is dissolved. In

DFT studies<sup>10</sup> a maximum adsorption energy of H<sub>2</sub>O on Fe(100) of -0.35 eV was calculated.

To estimate the rotation and translation abilities of the inhibitor on the iron surface, we calculate various adsorption sites and compare the energies to the most stable site of 2-butyne-1,4-diol on Fe(100). Two possible positions of the chemically similar acetylene molecule on the Fe(100) surface are mentioned in the literature: A fourfold hollow-site position was stated in cluster model calculations<sup>9</sup> as well as in HREELS experiments<sup>11</sup>, whereas more recent DFT-studies suggested a fourfold di- $\sigma$  geometry of acetylene on Fe(100)<sup>12,13</sup>.

The adsorbate-solvent interaction is further on analysed by adding a water molecule close to the unattached, and properly rotated hydroxyl group of the adsorbate to let hydrogen bonds form. The hydrogen bond strength is estimated to be in the order of 0.22 eV per molecule (=4.96 kcal/mol), which was found in a GGA-PBE DFT approach on H<sub>2</sub>O-dimers by Ireta<sup>14</sup>.

## II. COMPUTATIONAL METHODOLOGY

The calculations were performed with WIEN2k<sup>15</sup>, a software package for quantum mechanical calculations on periodic systems. We used the Perdew, Burke and Ernzerhof (PBE) 96 implementation of the generalized gradient approximation (GGA) for the exchange-correlation functional<sup>16</sup>. The augmented plane wave + local orbitals basis set (APW+lo) was applied for each atom. Core- and valence states were separated at an energy cutoff of -6.0 Ry, leading to Fe 1s-3s core states and Fe 3p, 4s and 3d valence states. The Fermi energy was calculated by k-space integration over the eigenvalues using a temperature broadening by a Fermi function with a broadening factor of 0.002 Ry, corresponding to room temperature.

Considering all reasonably occurring chemical bond lengths in this system and the plane wave convergence property of all atoms, the following Muffin tin radii (RMT) were chosen for the different atoms involved:

H: 0.53, C: 1.11, O: 1.29, Fe: 2.00 bohr

An RKmax cutoff parameter, *i.e.* the smallest RMT radius times Kmax, the magnitude of the largest K vector in the plane wave expansion, of 2.5 for systems containing hydrogen was chosen and increased up to 9.43 for calculations on pure Fe systems, since it has to be adapted to the smallest RMT, for comparable convergence. Unit cells of molecules without any Fe atoms were calculated with 1 k-point, whereas in surface slab calculations with a surface area of 4x3 Fe unit cells, 3x4x1 k-points, resulting in 6 k-points in the IBZ, were used.

We used a theoretically determined Fe bcc lattice parameter of 5.36 bohr, which is about 1% smaller than the experimental value of 5.41 bohr<sup>17</sup>. The iron sheet was modelled by a 5-layered Fe surface slab, consisting of three different iron layers (surface, subsurface, bulk). We chose the spin magnetic moment in the atomic spheres (mmi) as a criterion for the number of layers needed for

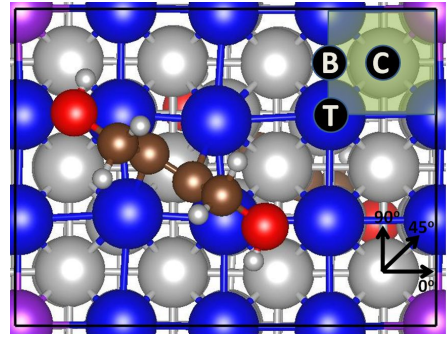


FIG. 1: Adsorption sites of 2-butyne-1,4-diol on the 4x3 super cell Fe(100) surface (top view). The green square represents the unit cell of Fe bcc. The C-C triple bond is in a bridged position (B), on top (T) of a surface Fe atom or in the center (C) of a Fe-square with angles of 0°, 45° and 90° to the Fe[100] direction. The image shows the most stable configuration "Center optimum".

accurate calculations with a still small computational effort. The calculated mmi of Fe(bcc) bulk atoms is  $2.2 \mu_B$ , whereas in a slab geometry the mmi of surface atoms is higher and varies towards the bulk, according to the so-called Friedel oscillation. For a 5-layer / 7-layer system we calculated mmi values of 3.0, 2.4, 2.6, 2.4, 3.0  $\mu_B$  / 3.0, 2.4, 2.5, 2.4, 2.5, 2.4, 3.0  $\mu_B$ . The surface and the subsurface layer is converged (constant mmi values of 3.0 and 2.4  $\mu_B$ ). Since only the electronic structure of these two layers play a role in the adsorption process, five iron layers were sufficient and calculation time could be saved.

The iron layers were separated from their periodic images by a vacuum region of ca. 26 bohr in z-direction. Relaxation resulted in a lifting of the surface layer of ca. 0.06 bohr (corresponding to 1% the lattice parameter) towards the vacuum region. The subsurface layer lifted ca. 0.02 bohr in the same direction (0.4% the lattice parameter).

In between the vacuum region the adsorbent was placed at three possible adsorption sites on the supercell surface, which is shown in figure 1. The sites (B, T, C) were determined by the position of the C-C triple bond, which was either at a bridged position (B), on top (T) of a surface Fe atom, or in the center (C) of a Fe atoms square. Angles of 0° and 45° (and 90° for B) of the triple bond with respect to the Fe[100] direction were chosen.

For each configuration we performed geometry optimisation, until a total force convergence criterion of 1 mRy/bohr was met and the adsorption energy ( $E_{ads}$ ) was determined by

$$E_{ads} = E_{adsorbed} - (E_{Fe} + E_{molecule}),$$

where  $E_{adsorbed}$  is the total energy of the system which has a molecule adsorbed to the Fe surface (as of now called "adsorbed system"),  $E_{Fe}$  the total energy of the pure Fe slab (as of now called "clean Fe surface") and  $E_{molecule}$  the total energy of the non-adsorbed molecule (as of now called "free molecule"). To obtain compara-

ble results, the individual energies were calculated by unit cells of the same size, compatible RKmax values and identical k-meshes (except for the free molecule, where only 1 k-point was sufficient).

### III. RESULTS AND DISCUSSION

This section divides into analysis of the adsorption geometry and the description of the electronic structure.

#### A. Geometry

The adsorption of 2-butyne-1,4-diol to the Fe(100) surface is found through the unsaturated carbon atoms, rather than the OH-group, due to the attraction of the alkyne group and the simultaneous repulsion of the hydroxyl groups. Consequently, Lendvay-Györik's findings on the preferred binding of the alkynol molecule 1-propyn-3-ol via the alkyne group in Gaussian calculations<sup>2</sup> can be confirmed by surface slab calculations on another alkynol molecule 2-butyne-1,4-diol.

Results on the different alkyne group positions, according to figure 1, are listed in table I. The full relaxation on all the configurations result in negative adsorption energies, hence, all these configurations are stable adsorption geometries and give a local minimum in energy. In the course of this relaxation, the unsaturated bond position stays in place, only the bond length increases. Consequently, the variety of different stable configurations lets us assume that the adsorbed molecule can, on the one hand, perform translations (B-T-C) and rotations ( $0^\circ$ - $45^\circ$ ) with a certain energy input and, on the other hand, cover not only the Fe(100), but also other crystal planes.

Moreover, we see that, clearly distinct from the other positions, the centred configurations show highest adsorption energies (-2.05 eV and -2.42 eV) and the molecule is closer to the Fe surface (lower h(C-Fe) values). The very optimum geometry "Center optimum" derives from full relaxation of the most favourable position "Center 45°" and the associated twist of the unsaturated bond (figure 2 and 1; total force convergence criterion:  $1 \text{ mRy/bohr}$  and energy convergence criterion:  $0.005 \text{ Ry}$ ). The structure is characterised by a fourfold di- $\sigma$  adsorption geometry with a slightly shifted angle of almost  $45^\circ$  to the Fe[100] direction (see figure 1 - top view). Thus, the adsorption geometry of 2-butyne-1,4-diol confirms to acetylene on Fe(100), as published in previous DFT studies<sup>12,13</sup>. The calculated adsorption energy of -2.70 eV/molecule is almost 8 times higher than for water on Fe(100) (-0.35 eV)<sup>10</sup>, which explains the inhibiting effect of 2-butyne-1,4-diol on steel.

For the purpose of investigating the adsorbate-solvent interaction ( $\text{H}_2\text{O}$ ), we first quantify the energy expense for the required rotation of the unattached hydroxyl

TABLE I: Adsorption geometries of 2-butyne-1,4-diol on Fe(100): adsorption energies ( $E_{ads}$ ), bond lengths (r) and vertical height distances (h) between the molecule and the iron surface; total force convergence criterion:  $1 \text{ mRy/bohr}$ ; "Center optimum": The angle decreases from  $45^\circ$  through further optimisation of "Center 45°".

Position	$E_{ads}$ [eV]	r(C-Fe) [Å]	h(C-Fe) [Å]
Bridge $0^\circ$	-1.02	2.12	1.57
Bridge $45^\circ$	-1.10	1.94	1.69
Bridge $90^\circ$	-1.17	1.92	1.95
Top $0^\circ$	-0.89	1.93	1.82
Top $45^\circ$	-1.00	1.91	1.79
Center $0^\circ$	-2.05	2.04	1.28
Center $45^\circ$	-2.42	1.95	1.49
Center optimum	-2.70	1.96	1.48

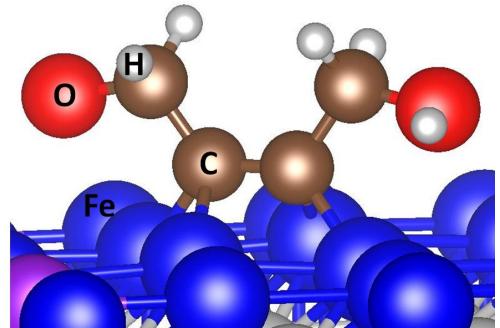


FIG. 2: Most stable geometry of 2-butyne-1,4-diol on the Fe(100) surface (Center optimum)

groups in the adsorbate. Rotation about the  $\alpha$ -bond axis towards the vacuum region lowers the optimum adsorption energy only about 2% ( $E_{ads}=-2.65 \text{ eV/molecule}$ ). However, rotating the hydroxyl group too close to the adsorbed molecule causes repulsive forces and lowers the stability about 16% (figure 3, image a,  $E_{ads}=-2.26 \text{ eV/molecule}$ ). Therefore, it should be easy to rotate the hydroxyl group about the  $\alpha$ -bond axis, but not too close to any other part of the adsorbed molecule.

In a second step, we rotate the OH group to a proper position for hydrogen bond formation and place a water molecule in the tetrahedral angle and the H atom in a distance of ca.  $2 \text{ Å}$  to the OH-group. Full relaxation results in an adsorption energy of  $E_{ads}=-2.86 \text{ eV/molecule}$  (figure 3, image b, total force convergence criterion:  $1 \text{ mRy/bohr}$ ). Thus, the  $\text{O}\cdots\text{H-O-H}$  hydrogen bond stabilises "Center optimum" by  $0.16 \text{ eV/molecule}$ , which approx. conforms to the usual hydrogen bond strength of  $0.22 \text{ eV}$  between two water molecules<sup>14</sup>. Hence, the unattached hydroxyl groups can interact with the aqueous solvent, while the inhibitor adsorbs via the alkyne group to the iron surface.

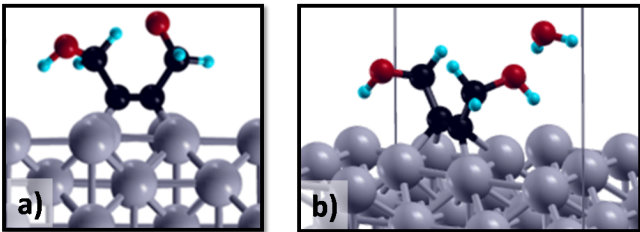


FIG. 3: a) The rotated OH group causes repulsive forces to the rest of the adsorbed 2-butyne-1,4-diol molecule on Fe(100) and lowers the stability compared to "Center optimum" b) A water molecule forms a hydrogen bond to the OH group in 2-butyne-1,4-diol, adsorbed on Fe(100), with the tetrahedral angle and a bond length of ca. 2 Å

Resolving the newly formed bond, we analyse the adsorbate's structure. The linear carbon skeleton of the free molecule, originating from the alkyne group, bends to an angled structure, as illustrated in figure 2. The resulting C-C-C angle of  $124^\circ$  is almost equal to the corresponding butenediol angle of  $125^\circ$ <sup>18</sup>, which would indicate a weakening of the triple bond into a double bond in the adsorbate. However, when looking at the C<sub>2</sub>-C<sub>3</sub> bond length, we observe an increase from 1.22 Å (triple bond in free molecule) to 1.41 Å (Center optimum) through adsorption. This bond length is shorter by 0.13 Å than the single bond in the free butanediol molecule<sup>19</sup> but longer by 0.07 Å than the double bond in free butenediol<sup>18</sup>. Also the C<sub>1</sub>-C<sub>2</sub> bond length has increased through adsorption, namely from 1.46 Å to 1.54 Å, which is exactly the bond length in free butanediol<sup>19</sup>.

## B. Electronic structure

Simply by structural analysis one cannot define the bond order in the adsorbate, thus, we investigate the electronic structure, in particular the density of states (DOS) of the free molecule (*but<sub>free</sub>*), the adsorbed molecule (*but<sub>ads</sub>*) and certain surface Fe atoms. First, figure 4 illustrates the total DOS of the adsorbed (a) and the free (b) molecule, which are determined by molecular orbitals (MOs) and therefore broadened by a Gaussian with a half-width of 0.0035 Ry. Comparing the red and black line, we observe a change in the MO scheme due to adsorption, which allows to analyse the electronic interactions between the molecule and the substrate. The two lines are horizontally shifted by 0.35 Ry, taking the MO at -1.45 Ry (top axis) as a reference point, where the 3D-electron density distribution remains unchanged after adsorption. Considering this shift, some red MO peaks are still slightly shifted in energy against the corresponding black MO peaks. This results from the geometric change of bond angles and bond lengths, as well as from the formation of new (chemical) bonds between adsorbate and substrate. Furthermore, the adsorbed molecule's states 1, 3 and 4 clearly show energy dispersion, such

as states in solids, while the others as well as the MOs of the free molecule are characterised by delta functions at certain energies.

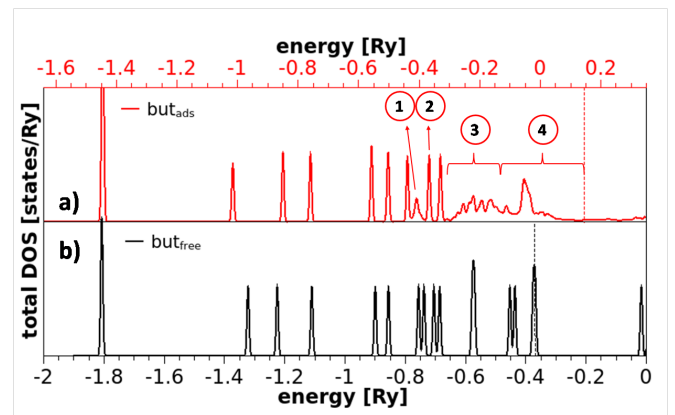


FIG. 4: Total DOS of adsorbed 2-butyne-1,4-diol on Fe(100), "Center optimum" configuration (a: red line) and free 2-butyne-1,4-diol (b: black line); energy scale aligned at the unchanging MO at -1.45 Ry (top axis) by 0.35 Ry; y-axis in arbitrary units; overlapping MOs with Fe substrate states are numbered (1-4)

The overlap of each of the four numbered states in figure 4 (a) with the Fe substrate electron density is illustrated in the enlarged DOS graphs in figure 5. At the top/bottom image the up-spin/down-spin Fe DOS (a/c) is compared to the up-spin/down-spin and total DOS (b/d) of the adsorbed molecule. We show two binding Fe surface atoms, namely Fe<sub>B1</sub> (solid, red line) and Fe<sub>B2</sub> (dashed, blue line) - see below in figure 6 - as well as the non-binding Fe<sub>NB</sub> atom, which is not involved in the chemical bond to the adsorbate and represents the unaffected iron substrate (gray area). Due to chemical binding, the Fe<sub>B1</sub> and Fe<sub>B2</sub> DOS overlaps with *but<sub>ads</sub>* in energy regions, where Fe<sub>NB</sub> doesn't.

The total electron density of these states (1-4) is further on visualised in 3D-iso surface plots of the adsorbed system in figure 6, where solid-red/dashed-blue arrows represent Fe<sub>B1</sub>/Fe<sub>B2</sub>. We see the interaction between C<sub>2</sub>/C<sub>3</sub> and Fe d-states of state 1 in image a. With a higher iso-value the C<sub>2</sub>-C<sub>3</sub>  $\pi$ -character of state 1 becomes clear in image b, which reveals a remaining  $\pi$ -character contribution to the adsorbed molecule's electronic structure. The d-character contributions of the two Fe<sub>Bx</sub> atoms to state 2 are illustrated in image c and state 3 is characterised by an electron density overlap to the Fe<sub>B1</sub> atoms (image d). The  $\pi$ -bond in the free molecule, which is characterised by the HOMO (image e), disappears at the analogous state 4 of the adsorbed molecule in favour of the formation of covalent bonds from the unsaturated carbon atoms to one Fe<sub>B1</sub> atom each (image f).

Furthermore, we look at the change in the cto - the total charge in the atomic spheres. The quantity depends on RMT, thus, one must not look at absolute numbers but relative values (comparing the adsorbed system

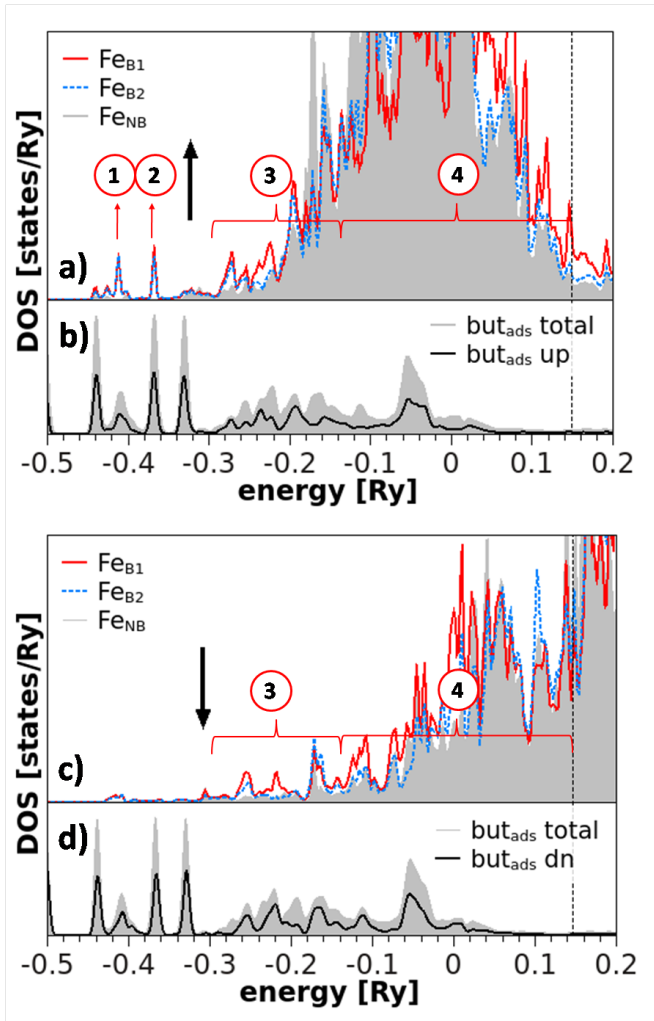


FIG. 5: Top: up-spin and bottom: down-spin DOS of the binding ( $\text{Fe}_{\text{B}x}$ ) and non-binding ( $\text{Fe}_{\text{NB}}$ ) iron surface atoms (a/c) of the "Center optimum" configuration compared to the up-spin (b)/down-spin (d) and the total DOS of adsorbed 2-butyne-1,4-diol on Fe(100)

with the clean Fe surface and the free molecule) indicate the charge transfer direction. The summed cto over all atoms in the molecule decreases by  $0.18 e$  due to adsorption. The main part is deducted from the unsaturated C atoms, which form the bonds to the Fe atoms (ca.  $0.07 e$  each). Corresponding to this decrease in the molecule, the cto increases on the two  $\text{Fe}_{\text{B}1}$  atoms by ca.  $0.08 e$  each, which sums up to ca.  $0.16 e$ . Consequently, charge is in good approximation transferred from the unsaturated C atoms in the molecule to mainly two Fe atoms and, in particular, to their d-orbitals. While the cto on the rest of the surface atoms stays constant, it decreases on the two  $\text{Fe}_{\text{B}2}$  atoms by ca.  $0.01 e$  each. The decreasing cto on these atoms indicates backbonding.

Since the explained charge transfer directly affects the magnetic moment of the spin polarised iron atoms and in particular the surface atoms, we analyse the mmi of

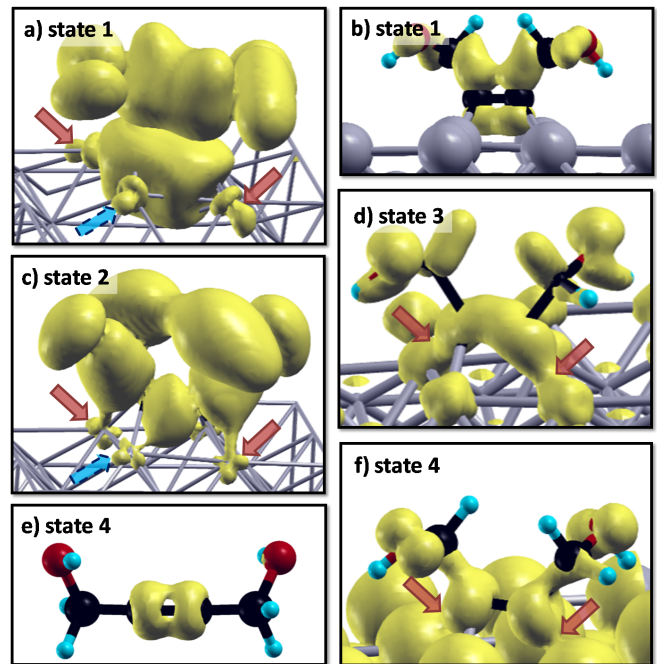


FIG. 6: States involved in the chemisorption of 2-butyne-1,4-diol on Fe(100). Solid-red arrows point at  $\text{Fe}_{\text{B}1}$  atoms, dashed-blue arrows at  $\text{Fe}_{\text{B}2}$  atoms. EIG: number of eigenvalues; state 1: EIG=1.5, a: iso-value=0.001, Fe d-states contribution are marked; b: iso-value=0.005, one can see the  $\text{C}_2/\text{C}_3$   $\pi$ -character; state 2: c: EIG=1.5, iso-value=0.001, arrows point at the Fe d-contributions; state 3: d: EIG=9.5, iso-value=0.03, the  $\text{C}_2/\text{C}_3$  -  $\text{Fe}_{\text{B}1}$   $\sigma$ -bonds are marked; state 4: the  $\text{C}_2$   $\pi$ -character MO in the free molecule (e: iso-value=0.06, EIG=2) vanishes in the adsorbed system (f: iso-value=0.08, EIG=76.5) in return of an overlap with  $\text{Fe}_{\text{B}1}$  (arrows).

the 5-layered surface slab. The average mmi over all Fe atoms of the three different layers are listed in table II of both the clean Fe surface (first column) and the adsorbed system (second column). In the third column the average decrease in the mmi (avg. mmi clean Fe surface - avg. mmi adsorbed system) is shown.

We observe Friedel oscillations, which is a damped mmi oscillation from the surface into the bulk, since the average mmi in both the clean Fe surface and the adsorbed system has its maximum in the surface layer, decreases in the subsurface layer and increases again in the bulk layer. Converged bulk layers should have an mmi of  $2.2 \mu_B$ , which would call for a thicker Fe slab. Through adsorption (third column) the mmi decreases in the surface layer, slightly increases in the subsurface layer and decreases again in the bulk layer, thus the adsorption causes additional damping.

The two  $\text{Fe}_{\text{B}1}$  atoms are most affected by an mmi decrease of ca.  $0.48 \mu_B$ . This is due to the occupation of additional Fe down-spin states with electron density from the molecule and the fact that the resulting decreased difference in the occupation of up- and down-spin states

TABLE II: Spin magnetic moment in the Fe atomic spheres (mmi) of the three different layers (surface, subsurface, bulk) of the 5-layered Fe surface slab, averaged over all atoms in the concerning Fe layer; first column: clean Fe surface; second column: adsorbed system (Center optimum configuration); third column: mmi decrease through adsorption of 2-butyne-1,4-diol

	avg. mmi clean Fe surface [ $\mu_B$ ]	avg. mmi adsorbed system [ $\mu_B$ ]	avg. mmi decrease [ $\mu_B$ ]
surface layer	2.915	2.799	0.12
subsurface layer	2.348	2.366	-0.02
bulk layer	2.562	2.525	0.04

corresponds to a smaller mmi. The  $\text{Fe}_{B2}$  atoms also show a large mmi drop of ca.  $0.15 \mu_B$ , compared to the average decrease in the surface layer of  $0.12 \mu_B$ .

#### IV. SUMMARY AND CONCLUSION

The corrosion inhibitor 2-butyne-1,4-diol chemisorbs covalently to the iron surface via the alkyne group. By Gaussian calculations Lendvay-Györik's<sup>2</sup> suggested the favoured adsorption of an alkynol molecule on one single Fe atom via the unsaturated group over the hydroxy O atom. These findings are confirmed in the present work by the more accurate model of a pe-

riodic solid Fe surface with WIEN2k on the alkynol 2-butyne-1,4-diol.

Two formed covalent bonds between 2-butyne-1,4-diol and the iron surface ( $\text{C}_2$  and  $\text{C}_3$  to two Fe atoms) primarily account for an adsorption energy of  $-2.65 \text{ eV}$  ( $\sim -255 \text{ kJ/mol}$ ). We also find smaller (backbonding) contributions of the other two Fe surface atoms in the  $\text{Fe}(100)$ -square to the electronic interaction with these two carbon atoms. Both the geometric properties and the presence of a  $\pi$ -character electronic state indicate a reduced double bond character in the adsorbate. A four-fold di- $\sigma$  adsorption geometry derives as the most stable configuration of 2-butyne-1,4-diol on  $\text{Fe}(100)$ .

Rotation and translation of the adsorbed molecule are energetically relatively inexpensive. Especially the hydroxyl group can almost freely rotate in the adsorbed molecule and interact with the aqueous solvent via hydrogen bonds. Since we find 2-butyne-1,4-diol to adsorb in the same geometry as acetylene on  $\text{Fe}(100)$ <sup>12,13</sup> and acetylene shows adsorption on each of the three crystal planes  $\text{Fe}(100)$ ,  $(110)$  and  $(111)$ <sup>9</sup>, we consequently expect adsorption on each of these planes. Thus, the steel surface with various differently oriented grains exposed can be covered areawide, which is necessary for effective corrosion inhibition.

#### Acknowledgments

This work was in cooperation with voestalpine AG and supported by the Christian Doppler Research Association (CDG).

- 
- <sup>1</sup> G. Gece, *Corrosion Science* **50**, 2981 (2008), ISSN 0010-938X.
- <sup>2</sup> G. Lendvay-Györik, G. Mészáros, B. Lengyel, and G. Lendvay, *Corrosion Science* **45**, 1685 (2003).
- <sup>3</sup> W. W. Frenier, V. R. Loop, and F. B. Growcock, in *Proc. 6th Europ. Symp. on Corrosion Inhibitors* (1985), pp. 183–198.
- <sup>4</sup> F. B. Growcock and V. R. Lopp, **28**, 397 (1988).
- <sup>5</sup> C. Fiaud, A. Harch, D. Mallouh, and M. Tzinmann, **35**, 1437 (1993).
- <sup>6</sup> M. Bartos, S. D. Kapusta, and N. Hackerman, *Journal of The Electrochemical Society* **140**, 2604 (1993), <http://jes.ecsdl.org/content/140/9/2604.full.pdf+html>.
- <sup>7</sup> K. Babic-Samardzija, C. Lupu, N. Hackerman, and A. R. Barron, *J. Mater. Chem.* **15**, 1908 (2005).
- <sup>8</sup> J.-M. Zhang, D.-D. Wang, and K.-W. Xu, *Applied Surface Science* **252**, 8217 (2006), ISSN 01694332.
- <sup>9</sup> A. B. Anderson and S. Mehandru, *Surface Science* **136**, 398 (1984), ISSN 0039-6028.
- <sup>10</sup> M. Eder, K. Terakura, and J. Hafner, *Physical Review B* **64**, 115426 (2001), ISSN 0163-1829, URL <http://link.aps.org/doi/10.1103/PhysRevB.64.115426>.
- <sup>11</sup> W.-H. Hung and S. L. Bernasek, *Surface Science* **339**, 272 (1995), ISSN 0039-6028.
- <sup>12</sup> P. Rochana and J. Wilcox, *Surface Science* **605**, 681 (2011), ISSN 00396028.
- <sup>13</sup> G.-D. Lee, S. Han, J. Yu, and J. Ihm, *Phys. Rev. B* **66**, 081403 (2002).
- <sup>14</sup> J. Ireta, J. Neugebauer, and M. Scheffler, *The Journal of Physical Chemistry A* **108**, 5692 (2004), ISSN 1089-5639.
- <sup>15</sup> P. Blaha, K. Schwarz, G. K. H. Madsen, D. Kvasnicka, and J. Luitz, *WIEN2K: An Augmented Plane Wave and Local Orbitals Program for Calculating Crystal Properties* (Vienna University of Technology, Austria, 2001).
- <sup>16</sup> J. P. Perdew, K. Burke, and M. Ernzerhof, *Phys. Rev. Lett.* **77**, 3865 (1996).
- <sup>17</sup> W. Martienssen and H. Warlimont, *Springer Handbook of Condensed Matter and Materials Data*, Springer handbook (Springer, 2006), ISBN 9783540304371.
- <sup>18</sup> Chemspider, *Csid:7774*, <http://www.chemspider.com/chemical-structure.7774.html/> (2013), URL <http://www.chemspider.com/Chemical-Structure.7774.html/>.
- <sup>19</sup> Chemspider, *Csid:13835209*, <http://www.chemspider.com/chemical-structure.13835209.html/> (2013), URL <http://www.chemspider.com/Chemical-Structure.13835209.html/>.